The QCD equation of state at finite density from analytical continuation

J. N. Guenther[1a,b], R. Bellwied[c], S. Borsányi[b], Z. Fodor[b,d,e], S. D. Katz[d],
A. Pásztor[b], C. Ratti[c], K. K. Szabó[e]

[a]*Department of Physics, University of Regensburg, Universitätsstraße 31, 93053 Regensburg, Germany*
[b]*Department of Physics, University of Wuppertal, Gaussstraße 20, 42119 Wuppertal, Germany*
[c]*Department of Physics, University of Houston, Houston, TX 77204, USA*
[d]*Institute for Theoretical Physics, Eötvös University, H-1117 Budapest, Hungary*
[e]*Jülich Supercomputing Centre, Forschungszentrum Jülich, 52425 Jülich, Germany*

Abstract

We want to study thermodynamical observables at finite density. Since direct lattice simulations at finite μ_B are hindered by the sign problem an efficient way to study the QCD phase diagram at small finite density is to extrapolate observables from imaginary chemical potential. In this talk we present results on several observables for the equation of state. The observables are calculated along the isentropic trajectories in the (T, μ_B) plane corresponding to the RHIC Beam Energy Scan collision energies. The simulations are performed at the physical mass for the light and strange quarks. μ_S was tuned in a way to enforce strangeness neutrality to match the experimental conditions; the results are continuum extrapolated and systematic effects are taken into account for the error estimate.

Keywords: lattice QCD, equation of state, phase diagram, finite density

1. Introduction

To analyse the quark gluon plasma that is created in heavy ion collision experiments at the LHC or RHIC a theoretical understanding of the quark gluon plasma in QCD is needed. In the region of the deconfinement transition lattice QCD is a good tool to study QCD since this area can not be accessed perturbatively. There have been several ideas in lattice QCD on how to obtain results at real finite chemical potential. However at the moment direct simulations that are continuum extrapolated and at physical quark masses are restricted to vanishing or imaginary chemical potential. On the other hand the collisions especially at RHIC take place away form the axis of zero chemical potential [1]. Therefore information in that region are needed. Even though it is not possible to do direct lattice simulations, it is possible to extrapolate observables form zero or imaginary chemical potential. This method is called analytical continuation.

In terms of the baryon chemical potential the pressure can be written as

$$\frac{P(\mu_B, T)}{T^4} = c_0(T) + c_2(T)\left(\frac{\mu_B}{T}\right)^2 + c_4(T)\left(\frac{\mu_B}{T}\right)^4 + c_6(T)\left(\frac{\mu_B}{T}\right)^6 + c_8(T)\left(\frac{\mu_B}{T}\right)^8 + O(\mu_B^{10}). \tag{1}$$
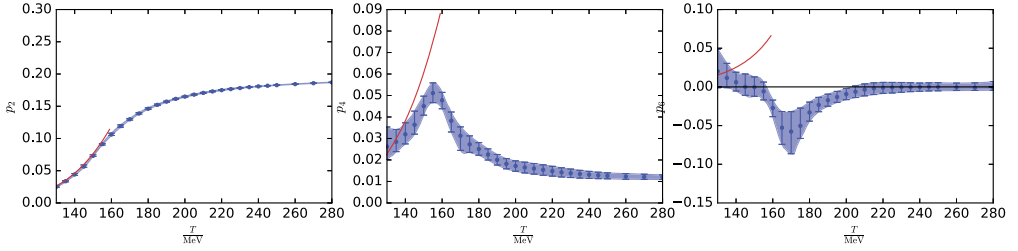
---

[1]speaker: Jana.Guenther@t-online.de

Fig. 1. The Taylor coefficients of the pressure. The red line shows the expectations of the HRG model.

In this proceedings we will present the continuum extrapolated Taylor coefficients of the pressure up to c_6 based on [2]. As well as the extrapolation for the transition temperature published in [3]. Our analysis is done with

$$\langle n_S \rangle = 0 \text{ and } \langle n_Q \rangle = 0.4 \langle n_B \rangle. \tag{2}$$

2. Analysis

Our lattice calculation uses the 4stout improved staggered action introduced in [4]. We use simulations on three different lattice size: $40^3 \times 10$, $48^3 \times 12$ and $64^3 \times 16$ and up to six different values for μ_B/T. As the simulations on the different lattice sizes correspond to slightly different temperatures and we want to know the derivative with respect to T, a first step in the analysis is the interpolation of $\langle \bar{\psi}\psi \rangle$, $\chi_{\bar{\psi}\psi}$ and χ_{SS} for the transition temperature and $\frac{n}{\mu_B T^2}$, $\frac{n_B}{\mu_B T^2}$ and $\frac{d\mu_Q}{d\mu_B}$ for the equation of state for every $\mu_B^{(j)}$.

The next step in the analysis is to fit the data in the $\hat{\mu}_B^2$ direction. For this we use three different fit functions to estimate the systematic error. In for imaginary μ_B all three fit functions can describe the data well. However their extrapolation to real μ_B can be different. The next step is the continuum extrapolation. We use a linear fit though the data from $N_t = 10, 12$ and 16. As an alternative analysis we also combine the the fit in the μ_B direction and the continuum extrapolation.

From the different fit functions we can determine the Taylor coefficients of the pressure. The results are shown in figure 1. The statistical error is determined via the bootstrap method with 1000 bootstrap samples. For the systematic error we use a histogram of all different analysises and take the central 68% thus employing the histogram method introduced in [5].

The fits can also be used to extrapolate to real chemical potential. The results for the transition temperature are shown in figure 2.

When extrapolating to real chemical potential the higher order coefficients become more important the further we extrapolate as can be seen from figure 3. From the Taylor coefficient we can calculate $\hat{n}_B$ to different orders. Using only the c_2 coefficient is a calculation up to $O(\mu_B)$ as the pressure has to be integrated over μ_B compared to $\hat{n}_B$.

Since we tuned our simulations to fulfill

$$\langle n_S \rangle = 0 \text{ and } \langle n_Q \rangle = 0.4 \langle n_B \rangle, \tag{3}$$

it is interesting to know how μ_Q and μ_S behave at real chemical potential for different values of μ_B. The results are shown in figure 4. These results can also be used in phenomenological calculations. For example some considerations that can be done with $\frac{d\hat{\mu}_Q}{dT}$ are presented in [6].

3. Acknowledgements

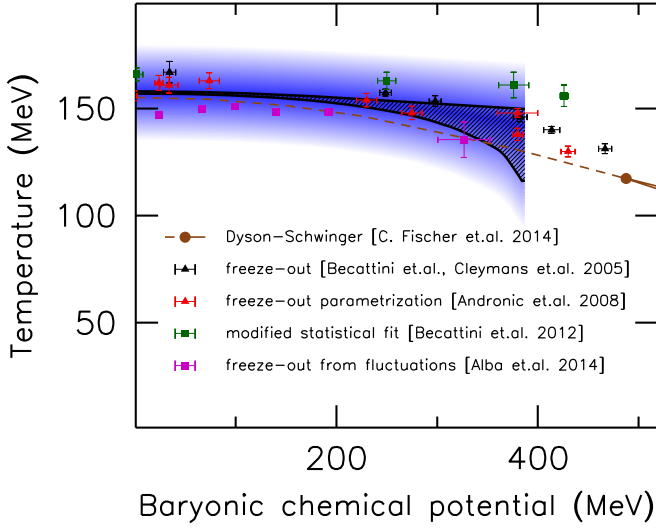Fig. 2. The phase diagram based on the μ-dependent T_c from the chiral condensate, analytically continued from imaginary chemical potential. The blue band indicates the width of the transition. The shaded black region shows the transition line obtained from the chiral condensate.
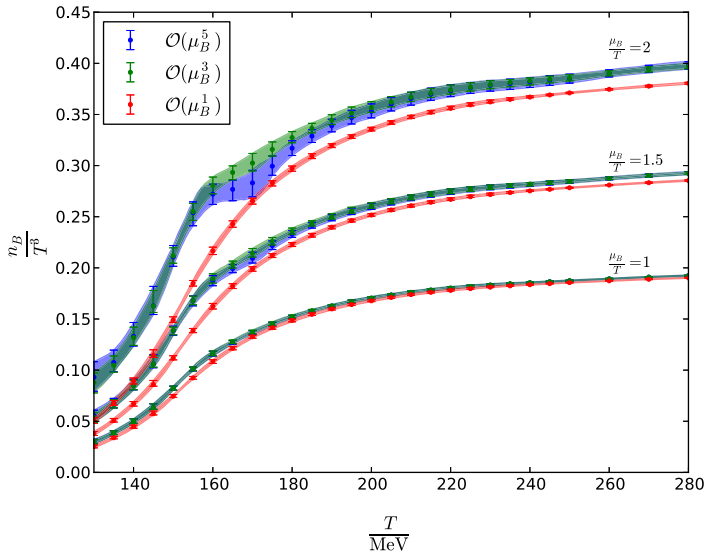

Fig. 3. The contribution of the different order coefficients to the baryon number for different values of μ_B/T
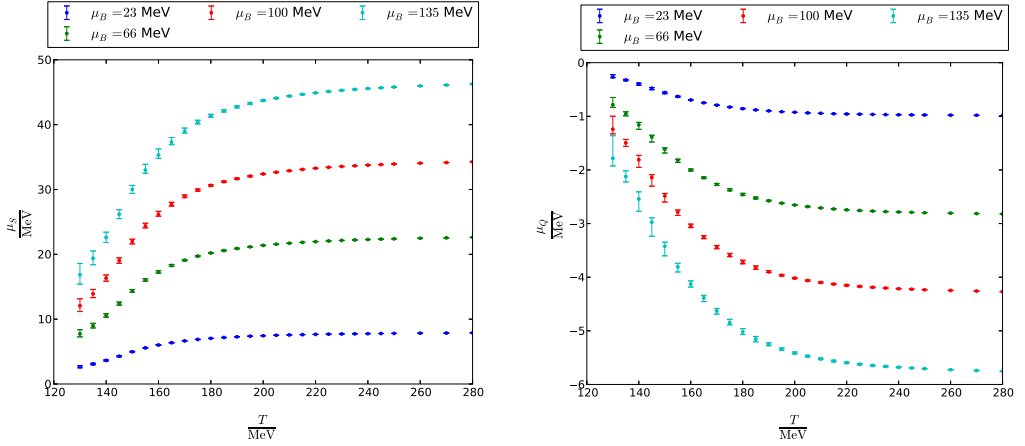
Fig. 4. μ_S and μ_Q at different values for μ_B with the condition $\langle n_S \rangle = 0$ and $\langle n_Q \rangle = 0.4 \langle n_B \rangle$

References

[1] G. Odyniec, Future of the beam energy scan program at RHIC, EPJ Web Conf. 95 (2015) 03027. doi:10.1051/epjconf/20149503027, 10.1051/epjconf/20159503027.

[2] J. Gunther, R. Bellwied, S. Borsanyi, Z. Fodor, S. D. Katz, A. Pasztor, C. Ratti, The QCD equation of state at finite density from analytical continuationarXiv:1607.02493.

[3] R. Bellwied, S. Borsanyi, Z. Fodor, J. Günther, S. D. Katz, C. Ratti, K. K. Szabo, The QCD phase diagram from analytic continuation, Phys. Lett. B751 (2015) 559–564. arXiv:1507.07510, doi:10.1016/j.physletb.2015.11.011.

[4] R. Bellwied, S. Borsanyi, Z. Fodor, S. D. Katz, A. Pasztor, C. Ratti, K. K. Szabo, Fluctuations and correlations in high temperature QCD, Phys. Rev. D92 (11) (2015) 114505. arXiv:1507.04627, doi:10.1103/PhysRevD.92.114505.

[5] S. Durr, et al., Ab-Initio Determination of Light Hadron Masses, Science 322 (2008) 1224–1227. arXiv:0906.3599, doi:10.1126/science.1163233.

[6] J. Noronha-Hostler, R. Bellwied, J. Gunther, P. Parotto, A. Pasztor, I. P. Vazquez, C. Ratti, Kaon fluctuations from lattice QC-DarXiv:1607.02527.

[7] Jülich Supercomputing Centre, Juqueen: Ibm blue gene/q supercomputer system at the jülich supercomputing centre, Journal of large-scale research facilities A1 (2015) 1. doi:http://dx.doi.org/10.17815/jlsrf-1-18.